2nd URSI AT-RASC, Gran Canaria, 28 May – 1 June 2018

Approximate Close-form Solution of Root-mean-square Delay Spread in Reverberation Chamber

Xiaotao Guo, Yichi Zhang, Meining Nie, Lifeng Wang, and Zilong Zhang
National Institute of Metrology, Beijing, 100029, http://www.nim.ac.cn

Abstract

In this study, reverberation chamber (RC) was used as a wireless channel simulator as root mean square delay spread (RMS-DS) between antennas was adjusted through applying different loadings. Based on the measurement and theoretical analysis, an approximate close-form solution has been developed to explain the quantitative relationship between the RMS delay spread and the parameters of loading. This solution has been proved to be valid in different loading conditions with a wider frequency band.

1. Introduction

Reverberation chamber (RC) has been extensively studied as electromagnetic compatibility (EMC) test equipment for many years. Recently it turns out to be a useful tool for wireless communication system study [1], especially for complex wireless system such as multiple-input–multiple-output (MIMO) system. As the impact of complex wireless channel on wireless communication system can be reproduced in RC when it has been used as the simulator, it is possible to evaluate the effective of complex wireless channel by over-the-air (OTA) test in RC [2].

Previous publications have shown that RMS-DS in RC will be changed when different absorbing materials or other loading applied [3-5], and the modification of quality factors is the physical principle of the adjustment in the chamber [6-8]. However, it is still challenging to calculate the quality factor of loading in practice. One possible solution is to predict the adjustment value rather than experimentally measurement after the adjustment.

In this study, we have developed an approximate close-form solution, which can quantificational explain the relationship between the value of RMS-DS and parameters of loading which will be applied in RC. This close-form solution would be beneficial for engineers who use RC as a simulator of complex wireless channel.

2. RMS-DS Adjusting

Details of devices parameters and materials used in experiment were introduced in Table. I. The VNA was firstly fixed to sweep from 800 MHz to 1 GHz, and 10001 points. Then, delay spread of the wireless channel was measured with a resolution of 5 ns and a maximum range of 50 μs. The loading conditions are noted by L0~L4, where L0 stands for the empty, and L1 ~ L4 stand for loading 1 ~ 4 piece(s) of absorbing material at the same location (Fig. 1).

Table 1. Detail of devices and materials

Name	Type	Parameters
RC	/	Size: 6.43 m × 5.09 m ×5.57 m
		Stirrers number: 2
		Working model: turn
		Turn steps: 100
TX	Schwarzbeck BBHA 9120 LF	Frequency range: 700MHz~6GHz
RX	Schwarzbeck SBA 9113	Frequency range: 500 MHz ~ 3 GHz
VNA	R&S ZVA8	Sweeping range: 800 MHz ~ 1 GHz
		Sweep points: 10001
Loading	VHP-12-NRL	0.2 m × 0.3 m× 0.3 m (cropped)

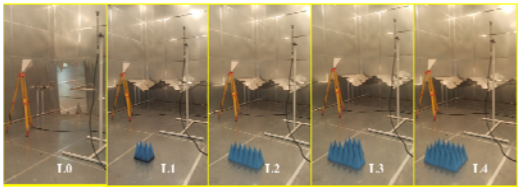

Figure 2. Different loading conditions of L0~L4.

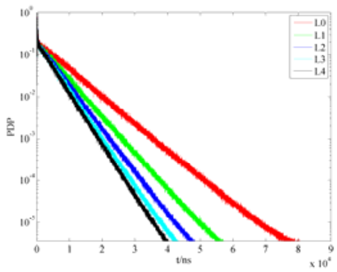

Figure 2. RMS-DS with different loading conditions in RC.

Table 2. RMS-DS in RC (800 MHz ~ 1 GHz)

Loading	L0	L1	L2	L3	L4
τ_{rms} (ns)	3592.9	2486.1	2119.8	1910.9	1792.2

The value of RMS-DS has decreased from 3592.9 ns to 1792.2 ns (table II.), while different loading conditions (L0~L4) were applied in the chamber respectively (Fig. 2). Each PDP value showed as a negative exponential form

[11], in accordance with the situation in rich-scattering channels.

3. Approximate Close-Form Solution

In order to eliminate this difference, an approximate close-form solution was developed based on the previous research [6,8,11].

1) In a rectangle resonance cavity, there is an average propagation time for each reflection path which is equal to $8V/cS$ [6], where c is the speed of light, V is the volume of cavity and S is the area of the surface of cavity.

As RC is not an ideal rectangle resonance cavity, the function of calculating average propagation time in RC was modified as (1)

$$t_{\text{ave}} \approx \xi \frac{8V}{cS} \quad , \tag{1}$$

where ξ is the correction factor of average propagation time for a certain RC.

The correction factor ξ should be less than 1 since there are two stirrers in our RC. The correction factor ξ was optimized to 0.88 by comparing the results calculated from close-form later expressed with the measurement with loading L1~L4. As the rate of volume of stirrers to cavity is 0.1159≈1-0.88. Thus, the optimizing of ξ is acceptable for our experiment.

PDP of wireless channel in RC could be explained by multi-attenuated-reflections as shown in Fig. 4. Statistically, power of electromagnetic signal will attenuate with certain factors after each reflection. Then PDP before and after each t_{ave} should be expressed as follows:

$$\text{PDP}\left(t+t_{\text{ave}}\right) \approx R \times \text{PDP}\left(t\right) \quad , \tag{2}$$

where R is the attenuation factor of each reflection.

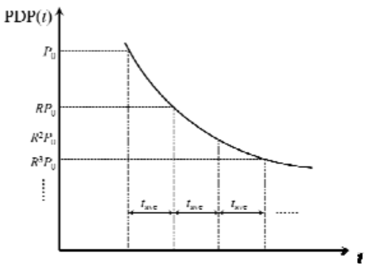

Figure 4. PDP explained by attenuated reflections.

2) Submitting (1)-(2) to $\text{PDP}(t) \approx \exp(-t/\tau_{\text{rms}})$, RMS-DS in RC can be calculated from R and t_{ave} as

$$\tau_{\text{rms}} \approx -\frac{t_{\text{ave}}}{\ln R} \quad . \tag{3}$$

For a certain RC, t_{ave} is a constant. Then the only parameter required for close form solution of RMS-DS in RC is the R under all kinds of loading conditions.

3) For the empty RC, attenuation factor of each reflection (noted by R_0) is mainly determined by imperfect boundary condition of the wall. In this study, the measurement results of loading L0 was used for calculating R_0 as

$$R_0 = \exp\left(-t_{\text{ave}}/\tau_{\text{rms}}^0\right) \quad . \tag{4}$$

4) For a loaded RC, attenuation factor of each reflection (noted by R_L) is decided by the empty chamber and the loaded absorbing material. Uniformity of electromagnetic field in RC determines that the reflections approximate evenly occur on the surface of wall. Therefore, attenuation factor with loading could be approximately calculated as follows:

$$R_{\text{L}} = R_0 \times \left(1 - S_{\text{L}}/S\right) \quad , \tag{5}$$

where S_L is the surface area of loaded absorbing material. The value of S_L is related to the style of placement, showed in Table III. While absorbing material is always placed on the floor and consisted by numbers of pyramid parts, S_L was calculated through adding its floor area and half of its side area.

Table 3. Placement of loading and value of surface area

Loading	Placement	S_L
L1	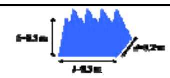	$S_1=l\times d+l\times h+d\times h$
L2	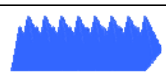	$S_2=2l\times d+2l\times h+d\times h$
L3	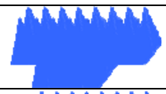	$S_3= S_1+ S_2-l\times h$
L4		$S_3= 2l\times 2d+2l\times h+2d\times h$

5) Submitting (5) to (3), RMS-DS in RC with arbitrary loading is approximated to be

$$\tau_{\text{rms}}^{\text{L}} \approx \frac{t_{\text{ave}}}{t_{\text{ave}}/\tau_{\text{rms}}^0 - \ln\left(1 - S_{\text{L}}/S\right)} \quad . \tag{6}$$

Theoretically, (1)-(6) stand for an approximate close-form solution of RMS-DS in RC which not only from the aspect of quality factor as Ref. [6,8,11], but also from the aspect of multi-attenuated-reflections. When complex wireless channel with certain RMS-DS is required to be simulated, parameters of loading could be estimated effectively with the support of (6).

Equation (6) can be rewritten as

$$S_{\mathrm{L}} \approx S\left[1-\exp\left(t_{\mathrm{ave}}/\tau_{\mathrm{rms}}^{0}-t_{\mathrm{ave}}/\tau_{\mathrm{rms}}^{\mathrm{L}}\right)\right]. \qquad (7)$$

Equation (19) can used to confirm the required amount of absorbing material loaded in the chamber when complex wireless channel in certain RMS-DS simulated in RC, like OTA test.

4. Validation of the Solution

With the support of (18), our approximate close-form solution of RMS-DS in RC with loading L1~L4 is in accordance with the measured result, as shown in Fig. 5. However, this is not enough to validate this close-form solution, since correction factor ξ in the approximate close-form solution is optimized based on the measured results, and some coincidence may occur as well (Fig. 5).

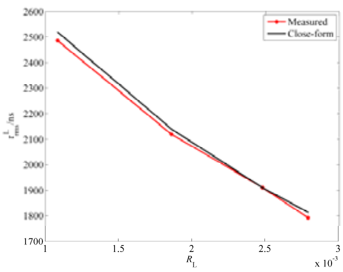

Figure 5. Approximate close-form solution of RMS-DS in RC with loading L1~L4 compared with measured result.

The first aspect of our validation was to check the RMS-DS in RC when loadings were at different positions. The key assumption of the approximate close-form solution is that the attenuation factor of each reflection is related to surface area of absorbing material but not to positions of loading, shown at (5).

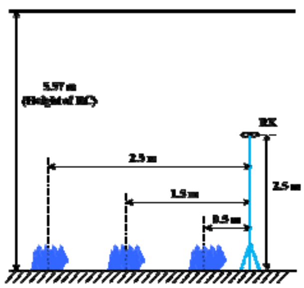

Figure 6. Positions of different loadings.

L1~L4 were repeated at three positions which were 0.5 m, 1.5 m and 2.5 m apart from the receiving antenna in the horizontal direction (Fig. 6). VNA was swept in the frequency bands from 800 MHz to 3 GHz, and RMS-DS was calculated in the frequency band 200 MHz. Therefore, central frequency of RMS-DS (f_c) in RC is 900 MHz to 2.9 GHz. RMS-DS in RC was similar when L1~L4 were repeated at different positions (Fig.7). This indicates that (5) in the close-form solution has been validated in measurement.

The second aspect of our validation is to verify that the close-form solution is valid not only in single frequency band of 200 MHz as in Fig.5, but also in a wider frequency band. As shown in Fig. 8, when L1~L4 was investigated in the frequency band from 800 MHz to 3 GHz, approximate close-form solutions of RMS-DS were generally conformed to the measurement results in the whole frequency band.

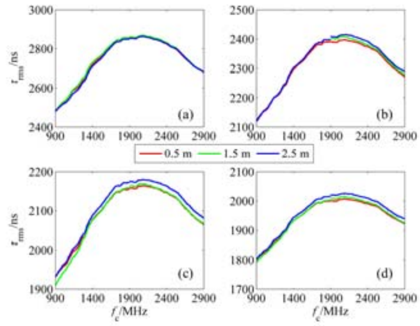

Figure 7. RMS-DS in RC with different loading positions: (a) for loading condition of L1; (b) of L2; (c) of L3; (d) of L4.

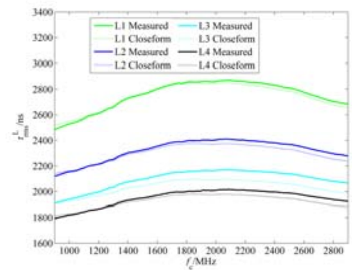

Figure 8. Approximate close-form solutions of RMS-DS in RC with L1~L4 and different loading conditions in frequency band of 800 MHz to 3 GHz is compared with measurement results.

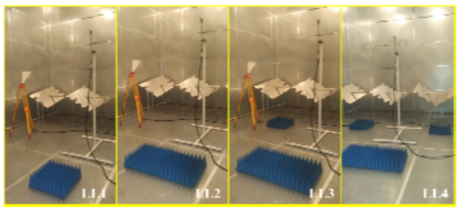

Figure 9. Different loading conditions of LL1~LL4 for RMS-DS simulation in RC.

The third aspect of our validation is to examine the close-form solution for other types of loading. In this case, absorbing material VHP-8-NRL was used to replace previous used material VHP-12-NRL. This absorbing material is not cropped and the size of each piece is 0.6 m × 0.6 m× 0.2 m. Larger loading conditions are noted by

LL1~LL4, standing for loading 1 ~ 4 piece(s) of absorbing material in the type of VHP-8-NRL. As shown in Fig. 8, when LL1~LL4 was investigated in the frequency band from 800 MHz to3 GHz, approximate close-form solutions of RMS-DS were also conformed to the measurement results in the whole frequency band.

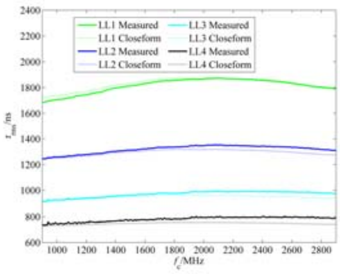

Figure 10. Results of approximate close-form solutions and measurement in RC Loading from LL1~LL4, frequency band from 800 MHz to 3 GHz.

5. Conclusion

In order to quantitatively simulate wireless channel with certain RMS-DS in RC, an approximate close-form solution has been developed to represent the relationship between the RMS-DS and the area of absorbing material loaded in the chamber. This close-form solution was developed based on the assumption of multi-attenuated-reflections for PDP in RC. The area of absorbing material was linked to the attenuation factor for each reflection, and the position of loaded absorbing material cannot influence RMS-DS simulation. In addition, by applying close-from solution in a wider frequency band (from 800 MHz to 3 GHz) and in different types of absorbing material, the estimated results were in accordance with measurement result. These experiments have validated the efficiency of the approximated close-form solution.

6. Acknowledgements

This work was supported by National Key Research And Development Plan of China (ID: 2017YFF0206201).

7. References

1. P. Corona, J. Ladbury, and G. Latmiral, “Reverberation-chamber research-then and now: a review of early work and comparison with current understanding,” *IEEE Transactions on Electromagnetic Compatibility*, **44**, pp. 87-94, 2002.

2. P. S. Kildal, C. Xiaoming, C. Orlenius, M. Franzen, and C. S. L. Patane, “Characterization of Reverberation Chambers for OTA Measurements of Wireless Devices: Physical Formulations of Channel Matrix and New Uncertainty Formula,” *IEEE Transactions on Antennas and Propagation*, **60**, pp. 3875-3891, 2012.

3. E. Genender, C. L. Holloway, K. A. Remley, J. Ladbury, G. Koepke, and H. Garbe, “Use of reverberation chamber to simulate the power delay profile of a wireless environment,” *2008 International Symposium on EMC Europe*, 2008

4. C. Xiaoming and P. S. Kildal, “Comparison of RMS delay spread and decay time measured in reverberation chamber,” *2010 Proceedings of the Fourth European Conference on Antennas and Propagation*, 2010.

5. C. Jung-Hwan, P. Seong-Ook, Y. Tae-Sik, and B. Joon-Ho, “Generation of Rayleigh/Rician Fading Channels With Variable RMS Delay by Changing Boundary Conditions of the Reverberation Chamber,” *IEEE Antennas and Wireless Propagation Letters*, **9**, pp. 510-513, 2010.

6. O. Delangre, P. De Doncker, M. Lienard, and P. Degauque, “Delay spread and coherence bandwidth in reverberation chamber,” *Electronics Letters*, **44**, pp. 328-329, 2008.

7. L. Bastianelli, L. Giacometti, V. M. Primiani, and F. Moglie, “Effect of absorber number and positioning on the power delay profile of a reverberation chamber,” *2015 IEEE International Symposium on Electromagnetic Compatibility*, pp. 422-427, 2015.

8. D. A. Hill, M. T. Ma, A. R. Ondrejka, B. F. Riddle, M. L. Crawford, and R. T. Johnk, “Aperture excitation of electrically large, lossy cavities,” *IEEE Transactions on Electromagnetic Compatibility*, **36**, pp. 169-178, 1994.

9. X. Guo, Z. He, Y. Zhang, X. Zhou, and M. Nie, “Investigation of field uniformity validation in reverberation chamber using VNA,” *2015 7th Asia-Pacific Conference on Environmental Electromagnetics*, pp. 270-273, 2015.

10. X. Guo, Z. He, Y. Zhang, X. Zhou, and M. Nie, “Theoretical uncertainty of RMS delay spread simulated by reverberation chamber,” *2015 12th International Conference on Electronic Measurement & Instruments*, pp. 270-273, 2015.

11. J. Hansen, “An analytical calculation of power delay profile and delay spread with experimental verification,” *IEEE Communications Letters*, **7**, pp. 257-259, 2003.

12. Z. Xin, Z. Zhong, B. Xin, L. Xiong, K. Guan, R. He, L. Ke, and W. Jianqiang, “Measurement uncertainty introduced by instruments in frequency domain channel measurement systems with a covariance-based analysis,” *2015 Asia-Pacific Symposium on Electromagnetic Compatibility*, pp. 302-305, 2015.

13. Testing and measurement techniques – Reverberation chamber test methods, *IEC Standard 61000-4-21*, 2011.